The Chemical Evolution of the Colour Systems Generated by Riccionidin A, 3-Deoxyanthocyanidins and Anthocyanins.

A. Alejo-Armijo, Johan Mendoza, A. Jorge Parola* and Fernando Pina*

LAQV, REQUIMTE, Department of Chemistry, College of Sciences and Technology, Universidade NOVA de Lisboa, 2829-516 Caparica, Portugal.

Abstract

The kinetics and thermodynamics (in acidic solutions) of the five chemical species reversibly interconnected by external stimuli, such as pH and light (multistate) generated by the liverworts colorant riccionidin A were investigated. The degradation products of the multistate formed after 10 days at neutral pH were identified.

The behaviour of the riccionidin A multistate was compared with previous results reported for the equivalent systems based on 3-deoxyanthocyanidins (found in mosses and ferns) and anthocyanins (ubiquitous in angiosperms). The five chemical species have *mutatis mutandis* similar structures in the three multistates. The most dramatic difference is the extremely slow interconversion rate between flavylium cation and *trans*-chalcone in riccionidin A and related compounds multistate (tens of days) when compared with deoxyanthocyanins (a few days) and anthocyanins (several hours) at room temperature. The mole fraction distribution of the five chemical species that constitute the multistate as a function of pH is also different in the three families of compounds. Some considerations regarding the chemical evolution of the three systems are given.

Graphical Abstract
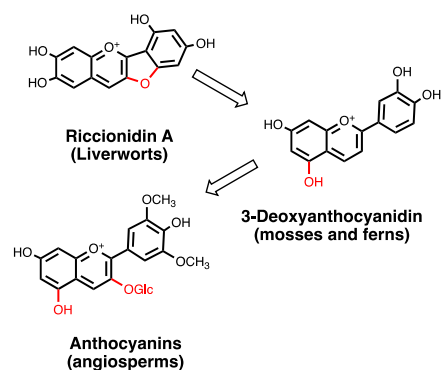
Rates of the inter-conversion between the species of the colour system: Riccionidin A (tens of days), 3-deoxyanthocyanins (a few days) and anthocyanins (several hours). No blue coloured species can be found unless in the anthocyanin's multistate.

Key words: Riccionidin A, auronidins, 3-deoxyanthocyanidins, anthocyanins, kinetics and thermodynamics, chemical evolution.

Introduction

Recently, Davies and Andersen[1] reported on the isolation and characterization of the compound auronidin-2'-neohesperidosideisolated from the liverwort *Marchantia polymorpha* (marchantia) and proposed the name auronidins for this family of compounds, Scheme 1. Like the aglycones of anthocyanins and 3-deoxyanthocyanins, riccionidin A is the aglycone of auronidin-2'-neohesperidoside, Scheme 1.

The structures shown in Scheme 1 regard only one of the chemical species (appearing under very acidic conditions) of a complex sequence of other compounds reversibly interconnected by external stimuli of pH, light and temperature, see below Fig.1.
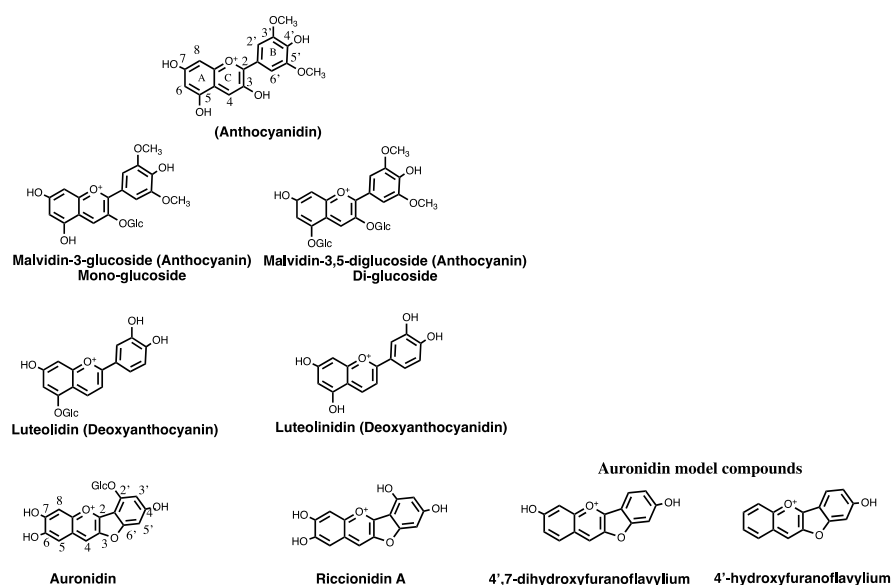
Scheme 1. Anthocyanins, 3-deoxyanthocyanins, auronidin and their respective aglycones together with two riccionidin A synthetic models (Glc=Glucose or other sugars, in the case of the reported auronidin is neohesperidoside).[1, ‡]

The scope of this work is to investigate the kinetics and thermodynamics of the multistate of riccionidin A (liverworts colorant) and compare with the similar multistates reported for 3-deoxyanthocyanidins (mosses and ferns colorants) and anthocyanins (angiosperms colorants).

State of the Art

Anthocyanins and deoxyanthocyanidins

---

‡ In reference 1 the first compound is named auronidin-4-neohesperidoside. In the present work, we use auronidin-2'-neohesperidoside to be consistent with flavylium derivatives numeration used throughout this work. The riccionidin A in reference 1 was also considered an auronidin.

Anthocyanins are the molecules that give red to blue colours to many flowers and fruits, but also leaves, vegetables, roots and stems.[2] The multistate generated by flavylium cations in aqueous solution was firstly investigated for anthocyanins but later was observed that it is also followed by anthocyanidins, deoxyanthocyanidins and related synthetic flavylium salts.[3,4,5,6,7] More recently it was reported that auronidin model compounds, see Scheme 1, follow in general the same multistate.[8,9]

In acidic to moderately acidic pH values, five pH dependent species are reversibly interconverted through four chemical reactions: proton transfer, hydration, tautomerization and *cis-trans* isomerization, Scheme 2. The anthocyanins multistate of chemical species (from here on designated as multistate) is characterized by its thermodynamics and kinetics. The thermodynamics can be accounted for by the respective energy level diagram,[10] Fig. 1a, or by a representation of the mole fraction distribution of the multistate species as a function of pH, Fig. 1b.[4]
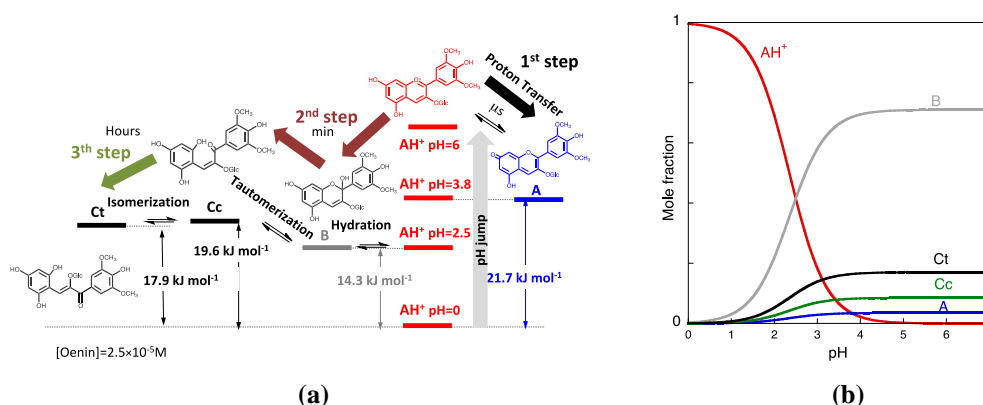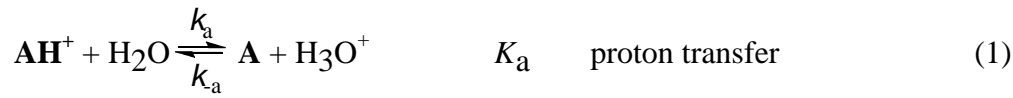

Figure 1. (a) Thermodynamic energy level diagram of malvidin-3-glucoside (oenin), $2x10^{-5}$ M showing the three kinetic steps upon a direct pH jump are shown; **(b)** mole fraction distribution of the species AH^+ and the neutral forms A, B, Cc and Ct at equilibrium.
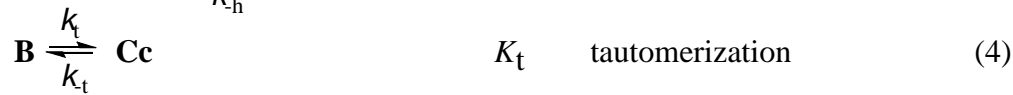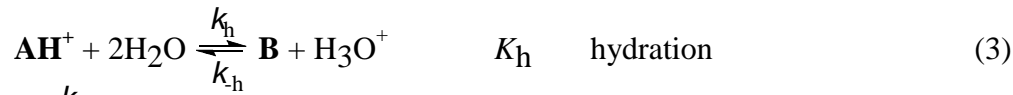
The kinetics of the anthocyanins multistate is most conveniently studied by addition of base to equilibrated solutions of the flavylium cation at pH≤1 (direct pH jumps) or by addition of acid to equilibrated solutions at higher pH values back to pH≤1 (reverse pH jumps). Stopped-flow is a very convenient tool to account for the fast kinetic steps. In a direct pH jump, three distinct kinetic steps take place. The first is proton transfer, eq.(1), that occurs in sub-microseconds, a rate which is faster than the dead time of the stopped-flow, eq.(2).[11] Considering that the following kinetic steps

are much slower, the species **AH⁺** (red colour) and **A** (purple colour) can be considered at equilibrium.

$$\textbf{AH}^+ + \text{H}_2\text{O} \underset{k_{-a}}{\overset{k_a}{\rightleftharpoons}} \textbf{A} + \text{H}_3\text{O}^+ \qquad K_a \qquad \text{proton transfer} \qquad (1)$$

$$k_{1st(direct)} = k_a + k_{-a}[H^+] \qquad (2)$$

The second step corresponds to the disappearance of **AH⁺**/**A** to form the species **B** through the hydration reaction followed by a faster tautomerization to give **Cc**. Since hydration at the pH values accessed by direct pH jumps is much slower than tautomerization, the second step is kinetically controlled by the hydration. A particular aspect of the hydration reaction is that it takes place from **AH⁺** and not from **A** (which does not hydrate in acidic to moderately acidic solutions).[3] This achievement was a breakthrough reported by Brouillard and Dubois and it is fundamental for the comprehension of the multistate. Eq.(3) and eq.(4) together with eq.(5) account for this kinetic step. In eq.(5), χ represents the mole fraction distribution of **AH⁺** and **B** at the pseudo-equilibrium, see below.

$$\textbf{AH}^+ + 2\text{H}_2\text{O} \underset{k_{-h}}{\overset{k_h}{\rightleftharpoons}} \textbf{B} + \text{H}_3\text{O}^+ \qquad K_h \qquad \text{hydration} \qquad (3)$$

$$\textbf{B} \underset{k_{-t}}{\overset{k_t}{\rightleftharpoons}} \textbf{Cc} \qquad K_t \qquad \text{tautomerization} \qquad (4)$$

$$k_{2nd(direct)} = C_{AH^+}k_h + C_B k_{-h}[H^+] = \frac{[H^+]}{[H^+] + K_a}k_h + \frac{1}{1 + K_t}k_{-h}[H^+] \qquad (5)$$

At this point, a pseudo-equilibrium can be considered, because the last process is by far the slowest and the system evolves to the equilibrium with the species **AH⁺**, **A**, **B** and **Cc** having enough time to equilibrate between them.

The last step, controlled by the isomerization, is given by eq.(6) and eq.(7).

$$\textbf{Cc} \underset{k_{-i}}{\overset{k_i}{\rightleftharpoons}} \textbf{Ct} \qquad K_i \qquad \text{isomerisation} \qquad (6)$$
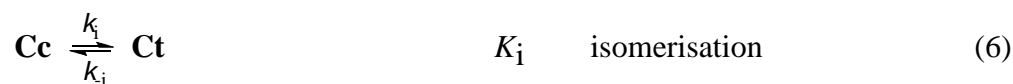
$$k_{3rd(direct)} = C_{Cc}k_i + k_{-i} = \frac{K_h K_t}{[H^+] + K_a + K_h + K_h K_t}k_i + k_{-i} \qquad (7)$$
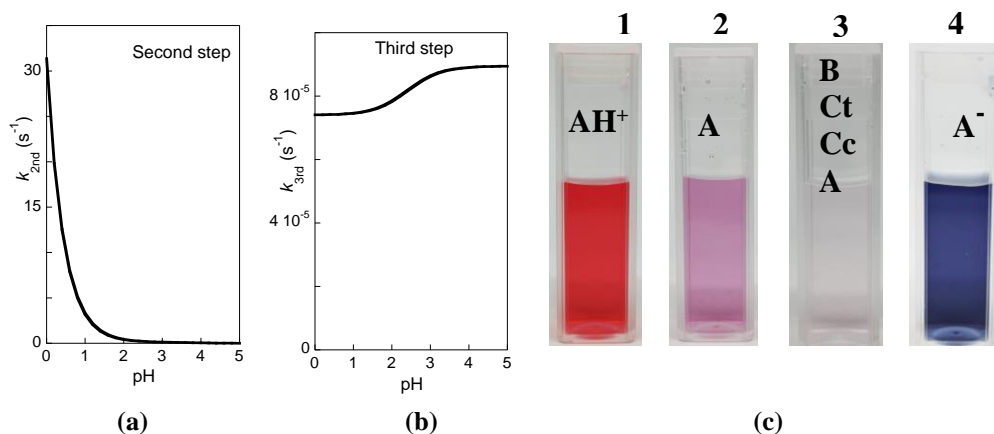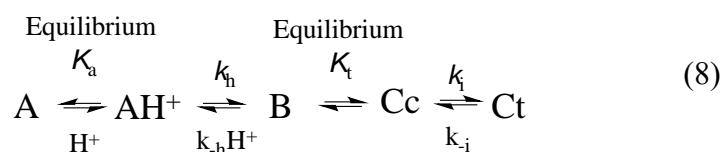
4

Figure 2. (a) Representation of the rate constants versus pH of the second step for Oenin 2.5×10^{-5} M, eq.(5); **(b)** the same for the third step, which is much slower, eq.(7). The rate and equilibrium constants to represent eq.(5) and eq.(7) were taken from reference [12]; **(c)** colours of Oenin 5.7×10^{-5} M multistate (1) Flavylium cation at pH=1.0; (2) quinoidal base immediately after a direct pH jump to pH=5.0; (3) at the equilibrium for the same pH of (2); (4) the intense blue is given by the anionic form of the quinoidal base as shown immediately after a pH jump to pH=8.0.

Comparison of the ordinate values of Fig. 2a and Fig. 2b confirms that the third step is several orders of magnitude slower in comparison with the second step. The colour of the flavylium cation is red, the quinoidal base is purple and the mono-cationic quinoidal base is blue, Fig. 2c. However, at the equilibrium the main species at higher pH values is the colourless hemiketal and the fraction of the purple quinoidal base is minor, see Fig. 1b and photo 3 in Fig. 2c.

3-Deoxyanthocyanidins

3-Deoxyanthocyanidins follow an identical multistate but there are several significant differences regarding the kinetics and the thermodynamics. In 3-deoxyanthocyanidins as well as in many other synthetic flavylium salts there is no *cis-trans* isomerization barrier and the pseudo-equilibrium does not take place, eq.(8).[7]

$$
\text{A} \underset{\text{H}^+}{\overset{K_a}{\rightleftharpoons}} \text{AH}^+ \underset{k_{-h}\text{H}^+}{\overset{k_h}{\rightleftharpoons}} \text{B} \overset{K_t}{\rightleftharpoons} \text{Cc} \underset{k_{-i}}{\overset{k_i}{\rightleftharpoons}} \text{Ct} \tag{8}
$$

This kinetic situation is equivalent to the equilibrium given by eq.(9), with X and Y representing respectively the equilibrium between **AH⁺** and **A** by one side, **B** and **Cc** by the other.

$$
\text{X} \underset{k_1}{\overset{k_1}{\rightleftharpoons}} \text{Y} \underset{k_2}{\overset{k_2}{\rightleftharpoons}} \text{Z}
$$
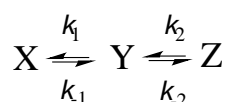
Applying the steady state hypothesis to Y, eq.(10) can be deduced.[7]

$$k_{bell} = \frac{\dfrac{[H^+]}{[H^+]+K_a} K_h K_t k_i + k_{-i}[H^+]}{[H^+] + \dfrac{k_i K_t}{k_{-h}}}$$

(10)

Eq.(10) gives a bell-shaped curve when represented as a function of pH. In Fig. 3, the bell shaped curve of luteolinidin, Scheme 1, is shown.
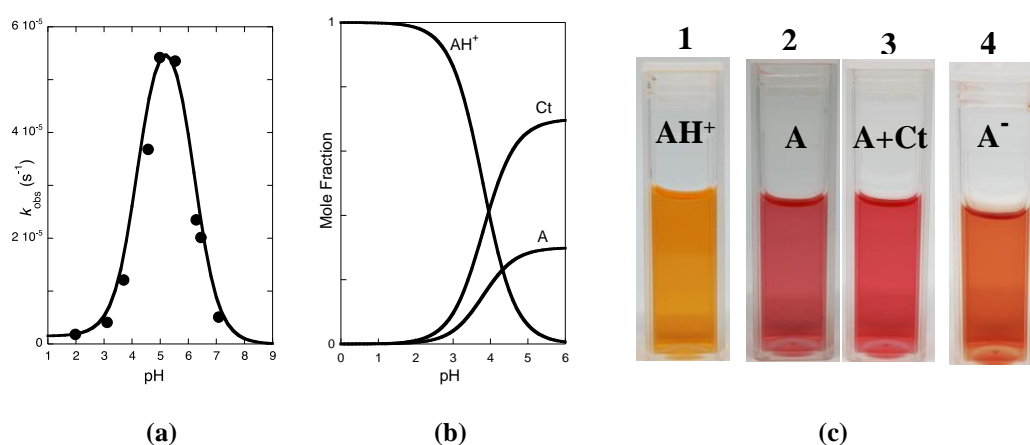

Figure 3. (a) Bell-shaped curve of the reaction towards the equilibrium versus pH of luteolinidin 2.5×10^{-5} M in ethanol:water (1:1). Fitting was achieved by means of eq.(10) for $K_h K_t K_i = 4 \times 10^{-9}$ $M^{-1}s^{-1}$; $K_t k_i / k_{-h} = 6.5 \times 10^{-7}$ $M^{-1}s^{-1}$; $k_{-i} = 1.5 \times 10^{-6}$ s^{-1}; $pK_a = 3.8$; (b) Mole fraction distribution of the species at the equilibrium, which is basically constituted by quinoidal base in equilibrium with trans-chalcone; (c) (1) Flavylium cation at pH=1.0, (2) quinoidal base immediately after a pH jump to pH=5; (3) at the equilibrium at pH=5; (4) immediately after a pH jump to pH=8.0. Immediately after a direct pH jump to pH=12 the colour is magenta (not shown).

It is worth noting for the following discussion that the flavylium cation of luteolinidin is yellow/orange and the quinoidal base is red. At the equilibrium the colour is given by a mixture of **Ct** (major species) and the red quinoidal base (minor species). This colour distribution is very different from the one of anthocyanins, Fig. 2c compared with Fig. 3c. Moreover, **B** and **Cc** are elusive species, observed during the kinetic studies but not present at the equilibrium. On the other hand, the ionized quinoidal base is dark orange. It is a matter of fact that no blue colour can be achieved with luteolinidin, even at more basic pH values.

Photoinduced cis-trans isomerization

One of the most interesting properties of the multistate is its photoinduced *trans-cis* isomerization, exemplified in Figure 4 for the model compound 4'-methoxyflavylium.[10]
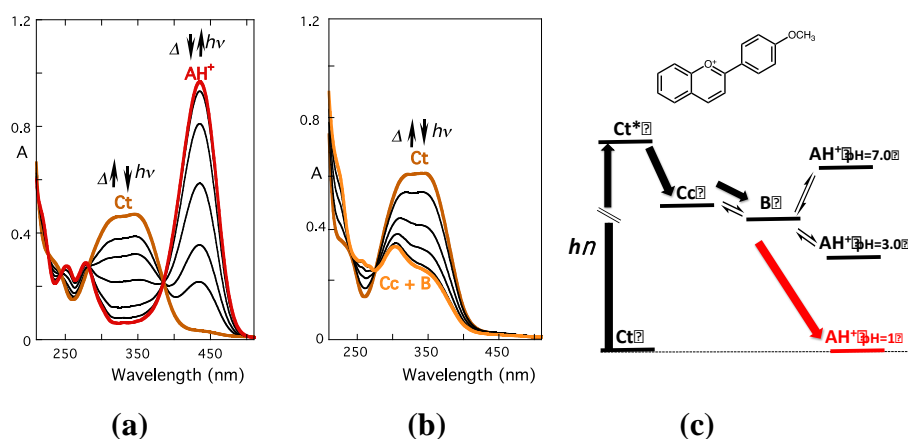

Figure 4. (a) pH 1.0, [Ct]= 2.5x10^{-5} M; the curves correspond to the irradiation times 0. 0.5, 1, 2, 4, 7 and 12 min; λ_{exc}=365 nm; **(b)** Spectral variations of 4'-methoxyflavylium at pH=7.0, [Ct]=3.2 x10^{-5} M; the curves correspond to the irradiation times 0, 0.25, 1.5, 3, 6, and 10 min; λ_{exc}=365 nm**; (c)** Energy level diagram of 4'-methoxyflavylium. Adapted from reference [10].

The compound 4'-methoxyflavylium possesses a very high *cis-trans* isomerization barrier and by consequence **Ct**, the stable species at higher pH values, is also metastable at pH=1.0. Consequently, irradiation of **Ct** at pH=1.0 leads to **Cc** that gives **B** (k_{obs}=0.95 s^{-1}) and this one produces flavylium cation (k_{obs}= 14 s^{-1}), Fig. 4a. In this case, there is no reversibility. Conversely, at pH=7.0 the flavylium cation is not thermodynamically accessed, Fig. 4c, and the photoproducts are a mixture of **Cc** and **B** (K_t=0.5), Fig. 4b. Reversibility back to **Ct** is observed.

In anthocyanins, the mole fraction distribution of **Ct** at the equilibrium is small and by consequence their photochromic systems are poor. However, in 3-deoxyanthocyanidins **Ct** is the major species and efficient photochromic systems have been described.[13]

Results and Discussion

Furanoflavylium molecules have long been prepared and identified as anthocyanins and related compounds, Scheme 3.[14] Some of these molecules are natural products such as Riccionidin A, identified in several liverworts as for example in the Antarctic *Cephaloziella varians*, in response to an abrupt increase of UVB radiation,[15] *in vitro* cultures of *Ricciocarpos natans*,[16] as well as in adventitious root cultures of the anacardiaceae *Rhus Javanica*.[17]

Related to this research, the kinetics and thermodynamics of riccionidin A model compounds 4',7-dihydroxyfuranoflavylium and 4'-hydroxyfuranoflavylium were reported.[8,9] It was proved that these auronidin model compounds follow the same multistate of species of anthocyanins where aurones are the *trans*-chalcones of the respective furanoflavylium salts, Scheme 2.[8]
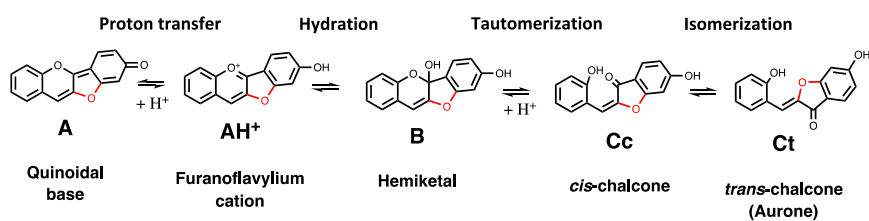
Scheme 2. Multistate of the chemical species of 4'-hydroxyfuranoflavylium in acid to moderately acidic medium.[8]

In spite of the similarities of furanoflavylium multistates with those of anthocyanins and deoxyanthocyanins, the rates for interconversion of the several species in auronidin model compounds are dramatically slower.[8,9] It is noteworthy the fact that the auronidin model compounds in Scheme 1 are better photoacids than the equivalent models of anthocyanins (without the furan bridge between rings B and C).[9] This means that furanoflavylium compounds are very appropriate molecules to dissipate by excited state proton transfer the electronic energy acquired upon light absorption.

The synthesis of riccionidin A was reported by Dyker and Bauer.[18] The suitable aldehyde and ketone were dissolved in acetic acid saturated with HCl gas at 100 ºC, to give initially the *trans*-chalcone, see experimental section for more details. The evolution of the synthesis was monitored taking an aliquot of 20 µl from the reaction vessel and dilute with 3 ml of 1:1 (v/v) methanol:HCl (0.2 M) solution, Fig. 5a. This result confirms the extremely slow conversion of the *trans*-chalcone into flavylium

cation, a result that was already observed by ^{1}H NMR and UV-vis absorption in model compounds of riccionidin A (furanoflavylium compounds), Scheme 1.[8,9]
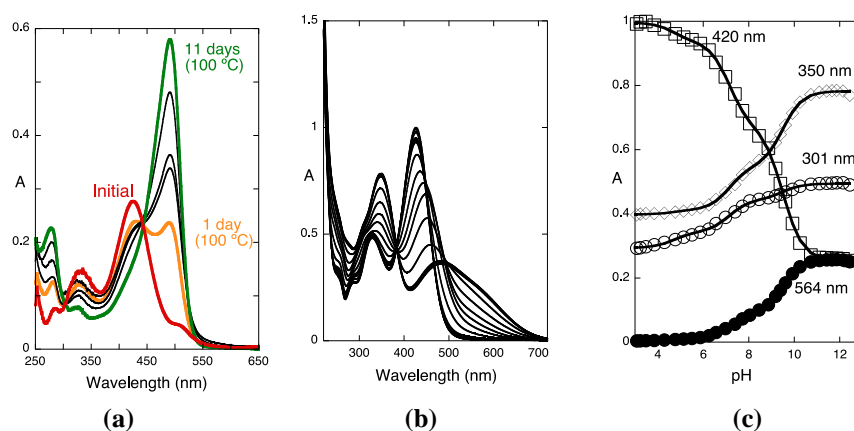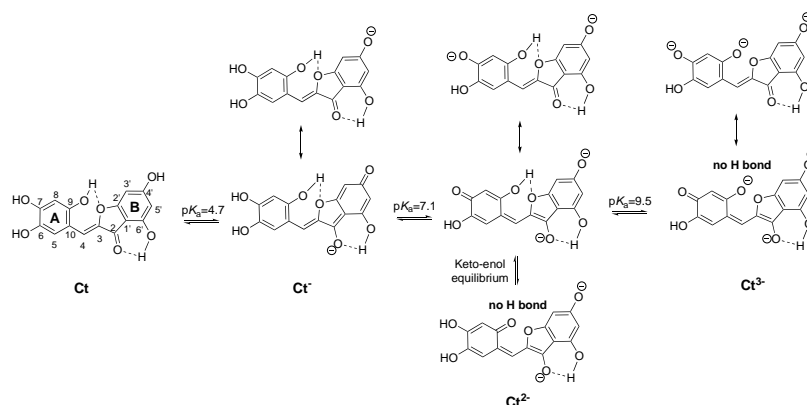

Figure 5. **(a)** Spectral variations during the synthesis of riccionidin A; **(b)** Spectral variations of *trans*-chalcone (immediately after the pH jump) as a function of pH, [Ct]=5.8 ×10^{-5} M; **(c)** Respective titration curves.

As shown in Fig. 5a the first spectrum (red spectrum) exhibits the characteristic absorption band of *trans*-chalcone and even at high temperature and very acidic conditions the flavylium cation is formed (green coloured) very slowly. The ^{1}H NMR of both species, *trans*-chalcone and flavylium cation, are in accordance to those reported in literature.[18]

The spectral variations of the *trans*-chalcone upon purification by column chromatography and taken immediately after direct pH jumps, Fig. 5b and Fig. 5c, are compatible with the existence of three acid-base equilibria tentatively identified in the scheme 3.

Scheme 3. Proposed protonation sequence for the *trans*-chalcone species. The numeration of the flavylium cation was used for comparison purposes.

9

The spectral variations during the *trans*-chalcones reaction at different pH values is shown in Fig. 6. In particular, at pH values in the interval 5<pH<7.5, a new species exhibiting a blue-shifted absorption bands, is formed, Fig. 6a. For longer reaction times the isosbestic points are lost indicating formation of other products not belonging to the multistate, below identified as decomposition products. The pH dependence of the rate constants before the appearance of these products versus pH can be interpreted considering a fitting obtained through eq.(11)

$$k_{obs} = a C_{ct} + b C_{ct-} + c C_{ct2-} + d C_{ct3-}$$

(11)

where C represents the mole fractions of the *trans*-chalcones in the different protonation states and the coefficients *a, b, c, d* the respective rate constants respectively, $a \approx b = 4.4 \times 10^{-6}$ s^{-1}, $c = 2.7 \times 10^{-3}$ s^{-1} and $d = 5.0 \times 10^{-3}$ s^{-1}.
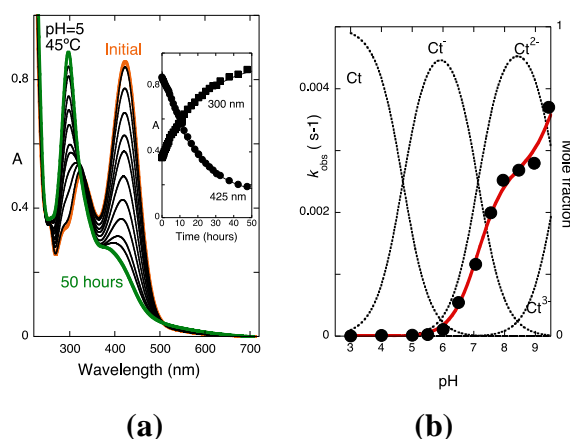

(a)   **(b)**

Figure 6. **(a)** Spectral variations of the *trans*-chalcone at pH=5.0 in methanol:water (1:1) at 45 °C, [Ct]=5.0 x10^{-5} M. The same behavior is observed in the pH range 1<pH<6.; **(b)** Variation of the observed rate constant as a function of pH; fitting was achieved for $a \approx b = 4.4 \times 10^{-6}$ s^{-1}, $c = 2.7 \times 10^{-3}$ s^{-1} and $d = 5.0 \times 10^{-3}$ s^{-1}. The last value is a rough estimation due to the decomposition process associated.

Considering that the first reaction towards formation of other products of the multistate is the isomerization of the chalcones, the rate dependence on the protonation state of the *trans*-chalcone can be explained with the help of Scheme 3. **Ct** species could be able to form up to two different intramolecular hydrogen bonds which confer an additional stability to the structure and difficult the *cis-trans* isomerization. Similarly, **Ct⁻** species can establish a hydrogen bond which also slows down the isomerization process. Differently is the case of **Ct²⁻** and **Ct³⁻** due to the

ionization of the A ring which promotes the breakdown of this last hydrogen bond and therefore facilitates the *cis-trans* isomerization.

More information regarding the riccionidin A multistate was obtained by HPLC-MS. The chromatographic profile as a function of time for the *trans*-chalcone form of riccionidin A is shown in Fig. 7 (0.5 mM at pH=7.1, in methanol:water (1:1), at room temperature). Peak 4 corresponds to the initial *trans*-chalcone. The m/z value of peaks 3 and 7 and the correspondent absorption spectra observed in HPLC-DAD are compatible with two other species of the multistate, respectively, hemiketal and *cis*-chalcone. Differently, neither peak 1 (m/z=319, negative mode), peak 2 (m/z=337, negative mode), peak 5 (m/z=154, negative mode) nor peak 6 (m/z=617, negative mode) are compatible with any expected component of the multistate. A proposed mechanism with structures compatible with these MS results is reported in Scheme 4.
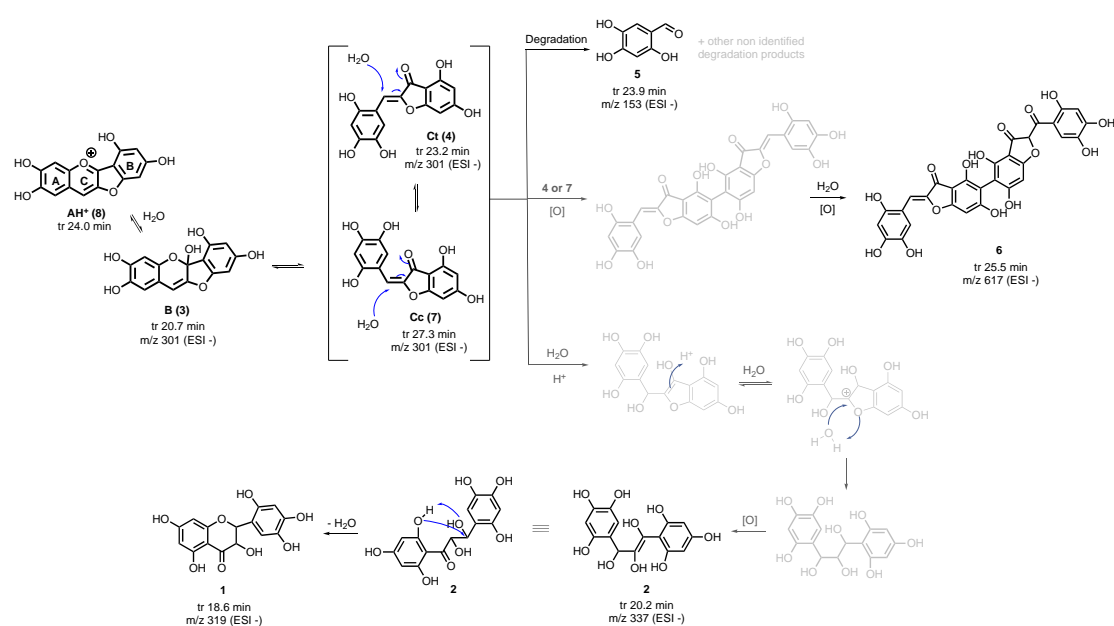
Scheme 4. Proposed chemical structures for peaks 1, 2, 5 and 6 detected by HPLC-MS and possible mechanistic pathways leading to their formation. The position of the methyl group was randomly assigned in the structure from peak 6.

The absorption spectra of the chromatographic peaks shown in Fig.7b contribute to the identification of the several chromatographic peaks. While peak 4 is unequivocally *trans*-chalcone, peak 7 is compatible with *cis*-chalcone: *i*) it is the first peak to appear after disappearance of peak 4, *ii)* the shape and position of the respective absorption spectra is the one expected for the *cis*-chalcone (slightly red-shifted and less intense when compared with **Ct**). On the other hand, the absorption

spectrum of peak 3, with a strong absorption in the UV, is compatible with the unconjugated hemiketal B. Peak 2, also with strong absorption in the UV, is compatible with a structure where conjugation is interrupted by a C sp^3 carbon, like in B. The fact that the peaks of B and Cc are well separated by HPLC indicates that the tautomerization reaction is also slower than in anthocyanins and *3*-deoxy-anthocyanins.
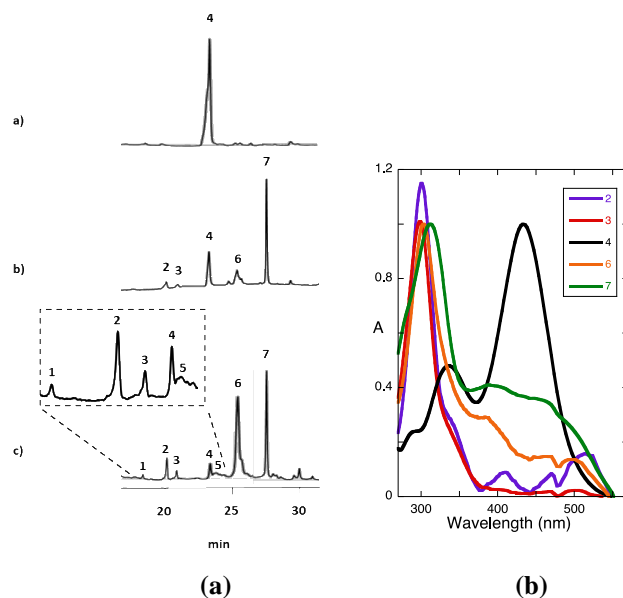

Figure 7. (a) Chromatographic profile of *trans*-chalcone (**4**) in methanol:water 1:1 (0.5 mM, pH = 7.1) at 300nm. a) freshly prepared; (b) after 4 days at r.t.; c) after 10 days at r.t. m/z=301 (negative mode) for peaks 3, 4 and 7; m/z=319 (negative mode) for peak 1; m/z=337 (negative mode) for peak 2; m/z=154 (negative mode) for peak 5; m/z=617 (negative mode) peak 6.

The photochemical reaction is another source of information for the system. In Fig. 8a, the spectral variations upon irradiation of **Ct** in acetonitrile containing a drop of trifluoroacetic acid are shown. The spectral variations shown in Fig. 8a clearly indicate the disappearance of **Ct**. The HPLC chromatograms taken at different irradiation times is presented are Fig. 8b. The initial process is, as expected, formation of *cis*-chalcone upon photoisomerization of Ct, accounting for the appearance of peak 7. The formation of peak 3 (hemiketal) from *cis*-chalcone can take place thermally or upon excitation of *cis*-chalcone via excited state proton transfer from Cc* to B* (tautomers). Peak 2 grows with 3 suggesting that structure 2 derives from 3 as proposed in Scheme 4.
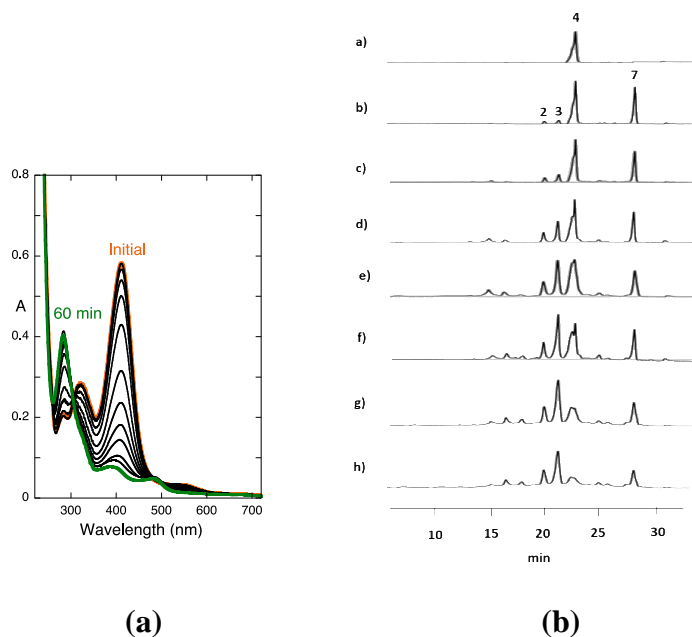
12

Figure 8. **(a)** Irradiation of *trans*-chalcone at 366 nm in acetonitrile (with a drop of TFA); [Ct]=3.4 x10^{-5} M; **(b)** Chromatographic profile of *trans*-chalcone solution (**4**) in acetonitrile (0.66 mM) at 300nm. a) before irradiation; b) after 6 min of irradiation (366 nm); c) after 16 min of irradiation (366 nm); d) after 35 min of irradiation (366 nm); e) after 1h of irradiation (366 nm); f) after 1h and 35 min of irradiation (366 nm); f) after 2h and 40 min of irradiation (366 nm); g) after 3h and 40 min of irradiation (366 nm).

Flavylium cation was also purified by column chromatography and a set of direct pH jumps were carried out to an extended range of higher pH values. The respective kinetic processes are very slow in all pH ranges and after a few hours no significant spectral variations were detected. However, depending on pH, spectral variations are observed after several days, see below. The pH dependent absorption spectra taken immediately after the direct pH jumps are shown in Fig. 9 and are compatible with a tetra-protonated acid, exhibiting well defined isosbestic points in four pH intervals.
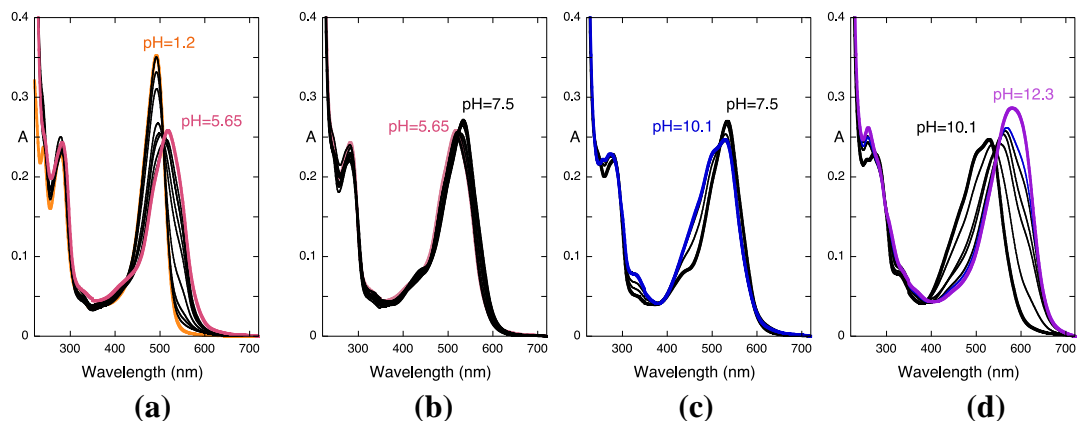
Figure 9. pH dependent spectral modifications of riccionidin A, $[AH^+]=3.3 \times 10^{-5}$ M upon pH jumps from pH = 1.0 to higher pH values in the following pH intervals: **(a)** 1.2<pH<5.65; **(b)** 5.65<pH<7.5; **(c)** 7.5<pH<10.1; **(d)** 10.1<pH<12.3.

This result was confirmed by the titration curves reported in Fig. 10a. Four inflection points were identified allowing determination of four pK_a values as expected from the four hydroxyl substituents of riccionidin A structure, Scheme 1.

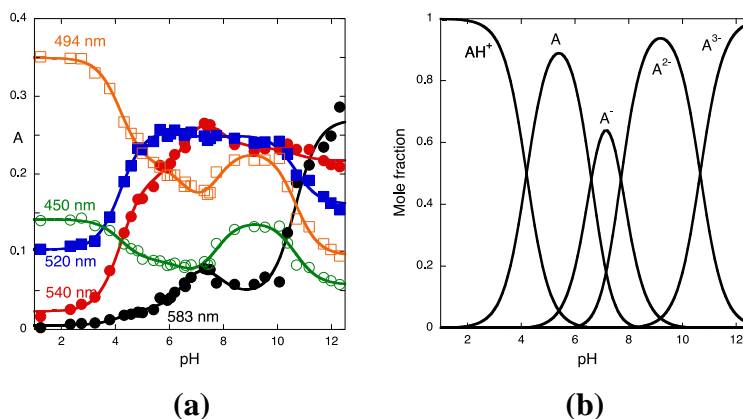|	
(a)	**(b)**

Figure 10. (a) Spectral variations of riccionidin A taken immediately after direct pH jumps from the flavylium cation equilibrated at pH=1.0. The system behaves as a tetra-protic acid with $pK_{a1}=4.2$; $pK_{a2}=6.6$; $pK_{a3}=7.7$; $pK_{a4}=10.7$; **(b)** pH dependent mole fraction distribution of the several species.

Once calculated the acidity constants, the mole fraction distribution of the several species that result from the deprotonation of the phenol groups of the flavylium cation is straightforwardly obtained, Fig.10b. A tentative protonation sequence is shown in Scheme 5, using as starting point the deprotonation sequence observed in the model compound 4,7-dihydroxyfuranoflavylium.[9]
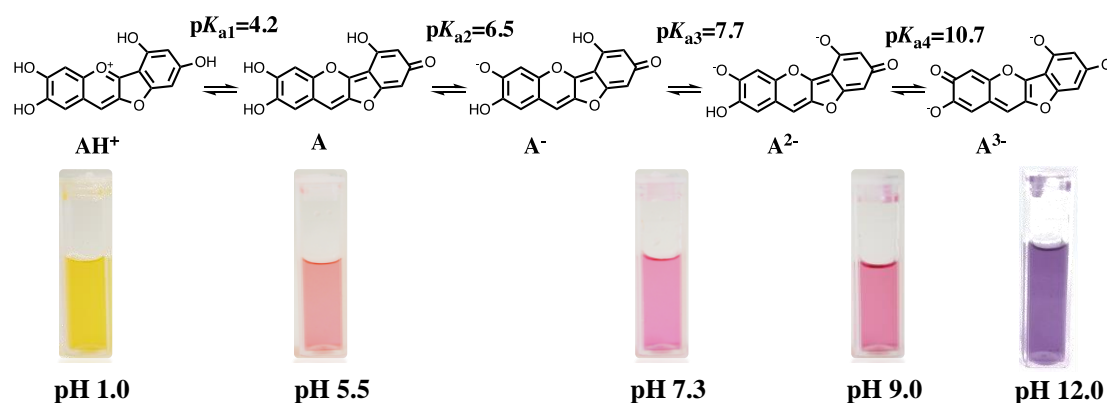
Scheme 5. Top: proposed deprotonation sequence for flavylium cation of riccionidin A; bottom: colour of the flavylium cation and quinoidal bases of **riccionidin A** immediately after the respective preparation. Only at extremely basic pH values a bluish-purple colour is observed. No blue colour like those of ionized quinoidal bases in anthocyanins was achieved.

Relevant information of the system regards the colour of the quinoidal base and flavylium cation, Scheme 5, down. Similarly to the natural auronidin[1] the red colour observed in riccionidin A is given by the quinoidal base.

Evolution of the initial absorption spectra reported in Fig. 9 is shown in Fig. 11. No significant spectral modifications were observed after 500 hours for pH<4, indicating that the flavylium cation is stable in that pH region. Fig. 11a, 11b and 11c show the spectral variations at three representative pH values where the species A, A$^-$ and A^{2-} are the major ones at zero time. In the three cases the kinetics are bi-exponential. The pH jump to pH=9.1 is extremely slow and some decomposition takes place.
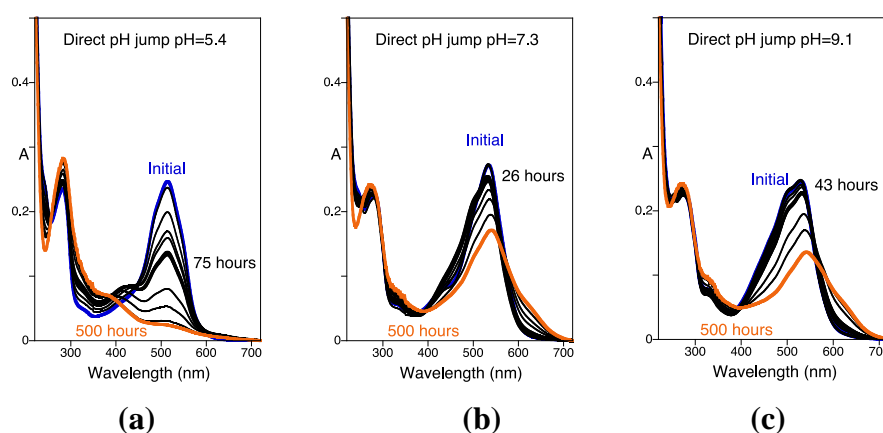

(a)   **(b)**   **(c)**

Figure 11. Kinetics of the direct pH jumps from flavylium cation at pH=1.0 at room temperature, $[AH^+]=3.3 \times 10^{-5}$ M.

At higher pH values the absorption spectra of the quinoidal bases is still observed. At pH=5.4 the absorption spectrum after 500 hours resembles those previously reported for peak 6 (see Scheme 4) in Fig. 7.

The reaction kinetics of flavylium cation solutions after a direct pH jump from pH=1.0 to pH=5.8 (taken at 45 ºC to decrease the reaction times), were followed by HPLC, Fig. 12. The mobile liquid phase of the elution gradient varies between 1<pH<2. Consequently, all quinoidal bases are transformed in flavylium cation. The HPLC profile after 10 minutes already shows a peak (peak 7) that we attributed to *cis*-chalcone. After 24 hours the *cis*-chalcone peak starts to decrease and peak 6 appears. The absorption spectrum of this peak is coincident with the one of Fig. 6a after 500 hours and Fig. 7b.
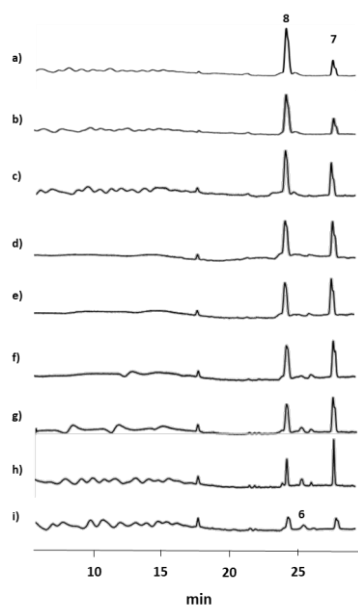
Figure 12. Chromatographic profile (at 300 nm) of flavylium salt (compound 8) solution (methanol:water 1:1; 1.15mM) after a pH jump to pH= 5.8 and at 45 ℃. a) after 10 min.; b) after 20 min.; c) after 1 h.; d) after 2 h.; e) after 4 h.; f) after 8 h.; g) after 24 h.; h) after 33 h.; c) after 48 h.

The data from Fig. 12 shows also that after 48 h the formation of more decomposition products are very significant. This prevents the definition of the equilibrium.

Conclusions

The plants where the three multistates have been found, respectively liverworts (auronidins), mosses and ferns (deoxyanthocyanins) and, angiosperms (anthocyanins) are in different positions in the evolution tree. The former are the older and the latter the newer. In the case of the multistate of the natural compound riccionidin A described through this work, as well as its synthetic model compounds, the most interesting feature is the extremely low rate of the interconversion between the several species of the multistate. This constitutes a handicap for the production of red colour by the plant in response to external stimuli. 3-Deoxyanthocyanidins multistate interconnect much faster than auronidins but still have a slower response when compared with anthocyanins. Neither auronidins nor deoxyanthocyanins multistates have species with blue colour, even in basic medium. Anthocyanins are more versatile in the colour pallet and the interconnection between the multistate species is much faster, permitting to respond more efficiently to natural external stimuli such as pH and light. This study complements from a chemical point of view the studies

developed from evolutionary plant biology and opens perspectives in the design and characterization of new pigments characterized by a high stability over an extended pH range when compared to anthocyanins.

Experimental Section

Materials and methods. All solvents and chemicals employed in syntheses and preparation of samples were reagent or spectrophotometric grade and were used as received; Millipore-grade water was used. NMR spectra were run on a Bruker Advance III 400 spectrometer (400 MHz for ^{1}H, 100 MHz for ^{13}C) at 298 K. High-performance liquid chromatography (HPLC) analyses were conducted on a Merck-Hitachi instrument equipped with a diode array detector (DAD), scan range 200–800 nm (Merck-Hitachi L-4500 Diode Array Detector), operating at 25 °C, using a reversed-phase analytical column (RP-HPLC, Purosphere® Star column, 250 mm×3 mm i.d., 5 μm). Samples were prepared in MeOH and the injection volume was 20 μL. The best peak separation was obtained with H_2O:$HClO_4$, 99.7:0.3, v/v (solvent A) and pure MeOH (solvent B) at a flow rate of 1 mL/min: 7% B for 2 min; linear gradient from 7% to 15% B for 6 min; linear gradient from 15% to 75% B for 17 min; linear gradient from 75% to 80% B for 2 min; linear gradient from 80% to 100% B for another 2 min; 100% B for 11 min and 5 min to return to the initial condition. The total run time excluding equilibration was 40 min. HPLC-MS analyses were performed in an Agilent 1200 Series equipment coupled with an Agilent 6130B Single Quadrupole detector with API-ES source. Column chromatography was carried out using Macherey-Nagel Polygoprep® 300-50C18. The column was packed with a mixture of stationary phase and H_2O:MeOH 80:20 v/v (pH=1.0). Gradient elution of increased MeOH proportion was performed to achieve separation. Separation was followed by HPLC and by fraction's weight.

Thermodynamic and kinetic studies. The pH jumps were carried out by adding a stock solution of flavylium salt or *trans*-chalcone in HCl 0.1M (1 mL) to a 3 mL quartz cuvette containing a solution of NaOH 0.1M (1 mL) and universal buffer of Theorell and Stenhagen (1 mL)[19] at the desired final pH. This defined the ionic strength as 0.1 M (controlled by the NaCl concentration resulting from neutralization). The final pH of the solutions was measured in a Crison basic 20 + pH meter. Spectroscopic measurements were performed using Mili-Q water with a constant temperature of 20±1 °C, with a Varian-Cary 100 Bio spectrophotometer.

Synthesis of (Z)-4,6-dihydroxy-2-(2,4,5-trihydroxybenzylidene)benzofuran-3(2H)-one (trans-chalcone of Riccionidin A) (3). The synthesis of compound **3** was achieved according to the experimental procedure previously described with some minor modifications. [20] Through a solution of 23 mg (0.15 mmol) of 2,4,5-trihydroxybenzaldehyde (previously prepared according to literature)[21] and 26 mg (0.16 mmol) of 4,6-dihydroxybenzofuran-3(2H)-one (previously prepared according to literature)[22] dissolved in 2 ml of acetic acid, dry hydrogen chloride was bubbled during 45 min at room temperature. After 24 h of additional stirring the mixture was purified by RP-column chromatography, yielding pure compound **3** (21 mg, 0.07 mmol, 50%). NMR data of compound **3** are in accordance with those reported in literature.[20] ^{1}H NMR (400 MHz, MeOD-d_4) δ 7.70 (*d, J* = 3.2 Hz, 1H), 7.22 (*d, J* = 3.2 Hz, 1H), 6.41 (*s*, 1H), 6.23 (*s*, 1H), 6.05 (*s*, 1H). ^{13}C NMR (100 MHz, MeOD-d_4) δ 183.4, 169.1, 168.5, 159.2, 153.2 (x2), 150.2, 147.4, 139.6, 118.5, 112.6, 108.1, 105.3, 104.4, 98.5, 92.0.

Synthesis of 2,3,6,8-tetrahydroxybenzofuro[3,2-b][1]benzopyrylium chloride (Riccionidin A; 2',4',6,7-tetrahydroxyfuranoflavylium chloride) (6). The synthesis of compound **6** was achieved according to the experimental procedure previously described with some minor modifications.[20] Through a solution of 60 mg (0.39 mmol) of 2,4,5- trihydroxybenzaldehyde (previously prepared according to literature)[21] and 65 mg (0.39 mmol) of 4,6-dihydroxybenzofuran-3(2H)-one (previously prepared according to literature)[22] dissolved in 4 ml of acetic acid, dry hydrogen chloride was bubbled during 45 min at room temperature. After 11 days of additional stirring at 100 ºC, the solution was allowed to cool to room temperature and 30 mL of Et$_2$O were added leading to the appearance of a dark solid. The precipitate was filtered off and carefully washed with Et$_2$O and dried, yielding flavylium salt **6** (0.103 g; 0.32 mmol; 82% yield). NMR data of compound **3** are in accordance with those reported in literature.[20] ^{1}H NMR (400 MHz, DMSO-d_6:TFA 4:1) δ 8.99 (*s*, 1H), 7.52 (*s*, 2H), 6.66 (*s*, 1H), 6.54 (*s*, 1H).

Acknowledgments

References

[1] H. Berland, N. W. Albert, A. Stavland, M. Jordheim, T. K. McGhie, Y. Zhou, H. Zhang, S. C. Deroles, K. E. Schwinn, B. R. Jordan, K. M. Davies, O. M. Andersen, *PNAS*, **2019**, *116*, 20232-20239.

[2] F. Pina, M. J. Melo, C. A. T. Laia, A. J. Parola, J. C. Lima, *Chem. Soc. Rev.*, **2012**, *41*, 869–908.

[3] R. Brouillard, J.-E. Dubois, *J. Am. Chem. Soc.*, **1977**, *99*, 1359-1364

[4] R. Brouillard, J. Lang, *Can. J. Chem.*, **1990**, *68*, 755-761.

[5] R. A. McClelland, S. Gedge, *J. Am. Chem. Soc.*, **1980**, *102*, 5838-5848.

[6] R. A. McClelland, G. H. McGall, *J. Org. Chem.*, **1982**, 47, 3730-3736.

[7] F. Pina, *J. Agric. Food Chem.,* **2014**, *62*, 6885-6897,

[8] A. Alejo-Armijo,. A. J. Parola,. F. Pina, *ACS OMEGA*, **2019**, *3*, 17853-17862.

[9] A. Alejo-Armijo, N. Basílio, A. Freitas, A. L. Maçanita, J. C. Lima, A. J. Parola, F. Pina, *Physical Chemistry Chemical Physics*, **2019**, *21*, 21651 – 21662.

[10] F. Pina, M. J. Melo, M. Maestri, R. Ballardini, V. Balzani, *J. Am. Chem. Soc.* **1997**, *119*, 5556-5561.

[11] A.L. Maçanita, P. F. Moreira, J. C. Lima. F. H. Quina, C. Yihwa, C. Voultier-Giongo *J. Phys. Chem. A*, **2002**, *106*, 1248-1255.

[12] F. Pina, A. J. Parola, M. J. Melo, J. C. Lima, V. de Freitas, chapter 2 in Anthocyanins from natural sources:exploiting targeted delivery for improved health, ed. M. S-L Brooks and G. B. Celli, Royal Society of Chemistry,U.K., 2019.

[13] M. J. Melo, S. Moura, A. Roque, M. Maestri, F. Pina, *J. Photochem. Photobiology,* **2000**, *135*, 33-39.

[14] G. Chakravarty, T. R. Seshadri, *Indian J. Chem.* **1964**, *2*, 319-323.

[15] K. R. S. Snell, T. Kokubun, H. Griffiths, P. Convey, D. A. Hodgson, K. K. Newsham, *Global Change Biology*, **2009**, *15*, 2563-2573.

[16] S. Kunz, H. Becker, *Z. Naturforsch*, **1955**, *50c*, 235-240.

[17] S. Taniguchi, K. Yazaki, R. Yabu-uchi, K. Kawakami, H. Ito, T. Hatano, T. Yoshida, *Phytochemistry*, **2000**, *53*, 357-363.

[18] G. Dyker, M. Bauer, *J. Prakt. Chem.,* **1998**, 340, 271-273.

[19] Küster, F. W.; Thiel, A.; Brückner, E. *Tabelle per Le Analisi Chimiche e Chimico-fisiche.* Hoepli: Milano, 1985; 157–160. The universal buffer used was prepared in the following way: 85% (w/w) phosphoric acid (2.3 mL), monohydrated citric acid (7.00 g), and boric acid (3.54 g) were dissolved in water; 1M NaOH (343 mL) was then added, and the solution was diluted to 1 L with water.

[20] G. Dyker, M. Bauer, *J. prakt. Chem.*, **1998**, *340*, 271-273.

[21] Y. H. Seo, K. Damodar, J. Kim, J. Jun, *Biorg. Med. Chem. Lett.* **2016**, *26*, 1521-1524.

[22] A. Meguellati, A. Ahmed-Belkacem, A. Nurisso, W. Yi, R. Brillet, N. L. Chavoutier, A. Fortuné, J.M. Pawlotsky, A. Boumendjel, M. Peuchmaur, *Eur. J. Med. Chem.* **2016**, *115*, 217-229.